

# Impaired Synapse Elimination during Cerebellar Development in PKC $\gamma$ Mutant Mice

Masanobu Kano,\* Kouichi Hashimoto,\* Chong Chen,†  
Asa Abeliovich,† Atsu Aiba,† Hideo Kurihara,‡  
Masahiko Watanabe,‡ Yoshiro Inoue,‡  
and Susumu Tonegawa†

\*Department of Physiology  
Jichi Medical School  
Minamikawachi-machi  
Tochigi-ken 329-04  
Japan

†Howard Hughes Medical Institute  
Center for Learning and Memory  
Center for Cancer Research  
and Department of Biology  
Massachusetts Institute of Technology  
Cambridge, Massachusetts 02139

‡Department of Anatomy  
Hokkaido University School of Medicine  
Sapporo 606  
Japan

## Summary

**PKC $\gamma$  is highly expressed in Purkinje cells (PCs) but not in other types of neurons in the cerebellum. The expression of PKC $\gamma$  changes markedly during cerebellar development, being very low at birth and reaching a peak around the third postnatal week. This temporal pattern of PKC $\gamma$  expression coincides with the developmental transition from multiple to single climbing fiber innervation onto each PC. In adult mutant mice deficient in PKC $\gamma$ , we found that 41% of PCs are still innervated by multiple climbing fibers, while other aspects of the cerebellum including the morphology and excitatory synaptic transmission of PCs appear normal. Thus, elimination of multiple climbing fiber innervation appears to be specifically impaired in the mutant cerebellum. We suggest that the developmental role of PKC $\gamma$  may be to act as a downstream element in the signal cascade necessary for the elimination of surplus climbing fiber synapses.**

## Introduction

Protein kinase C (PKC) is richly represented in neural tissues and has been implicated in a variety of neuronal functions, including modulation of ion channel activity and synaptic transmission (Tanaka and Nishizuka, 1994). Ten isoforms of PKC have been identified in mammalian tissues that differ in most biochemical properties and expression patterns (Nishizuka, 1992; Tanaka and Nishizuka, 1994). The  $\gamma$  isoform (PKC $\gamma$ ) is expressed solely in the neurons of the brain and spinal cord (Saito et al., 1988). Subcellular localization studies indicate that PKC $\gamma$  is present primarily in the soma and dendritic processes of neurons (Huang et al., 1988; Kose et al., 1988; Tanaka and

Saito, 1992). The expression of PKC $\gamma$  is developmentally regulated, being very low at birth and increasing progressively up to 2–3 weeks of age in the rat (Hashimoto et al., 1988).

Mice deficient in PKC $\gamma$  have modified long-term potentiation (LTP) in the hippocampus (Abeliovich et al., 1993a) and exhibit mild deficits in spatial and contextual learning (Abeliovich et al., 1993b). Furthermore, these mice are mildly ataxic and show a decreased effect of ethanol on behaviors (Harris et al., 1995; Chen et al., 1995 [this issue of *Cell*]). Since PKC $\gamma$  is highly expressed in cerebellar Purkinje cells (PCs) (Huang et al., 1988; Kose et al., 1988; Saito et al., 1988; Tanaka and Saito, 1992) and has been implicated in synaptogenesis (Herms et al., 1993; Moriya and Tanaka, 1994) and synaptic plasticity (Crepel and Krupa, 1988; Crepel and Jaillard, 1991; Linden and Connor, 1991; Linden, 1994; Hemart et al., 1995) in the cerebellum, we analyzed the development of the cerebellum in PKC $\gamma$  mutant mice. The effects of the PKC $\gamma$  deficiency on the synaptic mechanisms for motor coordination and for discrete motor learning are addressed in the accompanying paper (Chen et al., 1995).

PCs in the cerebellum receive distinct types of excitatory inputs from parallel fibers (PFs) and climbing fibers (CFs) (Ito, 1984; Palay and Chan-Palay, 1974). PFs consist of the bifurcated axons of granule cells and synapse onto the dendritic spines of PCs. Each PF synapse is weak, but one PC receives inputs from approximately  $10^6$  PF synapses. In contrast, CFs originate from the inferior olive and form strong excitatory synapses on proximal dendrites of PCs. In an adult mouse, each PC is innervated by a single CF. These two distinct types of excitatory synapses are generated and modified dynamically during postnatal development. During early postnatal rodent development, PCs are multiply innervated by CFs (Crepel, 1982): at postnatal day five (P5), three to four CFs innervate single PCs. Thereafter, PF–PC synapses are continuously generated concurrent with the migration of granule cells from the external granular layer to the internal granular layer. Massive elimination of supernumerary CFs occurs during the second and third postnatal weeks until a one-to-one relation between CFs and PCs is attained at approximately P21. This relation is then maintained through adult life. In situ hybridization analysis shows that the expression of PKC $\gamma$  in the cerebellum exhibits a peak during the third postnatal week (Herms et al., 1993; Moriya and Tanaka, 1994). This observation is consistent with the notion that PKC $\gamma$  plays a role in the elimination of CFs.

In this study, neither light nor electron microscopic observations revealed any anatomical abnormalities in the cerebella of PKC $\gamma$  mutant mice. Electrophysiological recordings indicated that both CF– and PF–PC synapses are functional. However, about 40% of PCs in mature mutant mice were multiply innervated by CFs. On the other hand, PF–PC synaptic transmission appeared normal. These results indicate that PKC $\gamma$  is a key molecule required for the elimination of surplus CFs during cerebellar development.

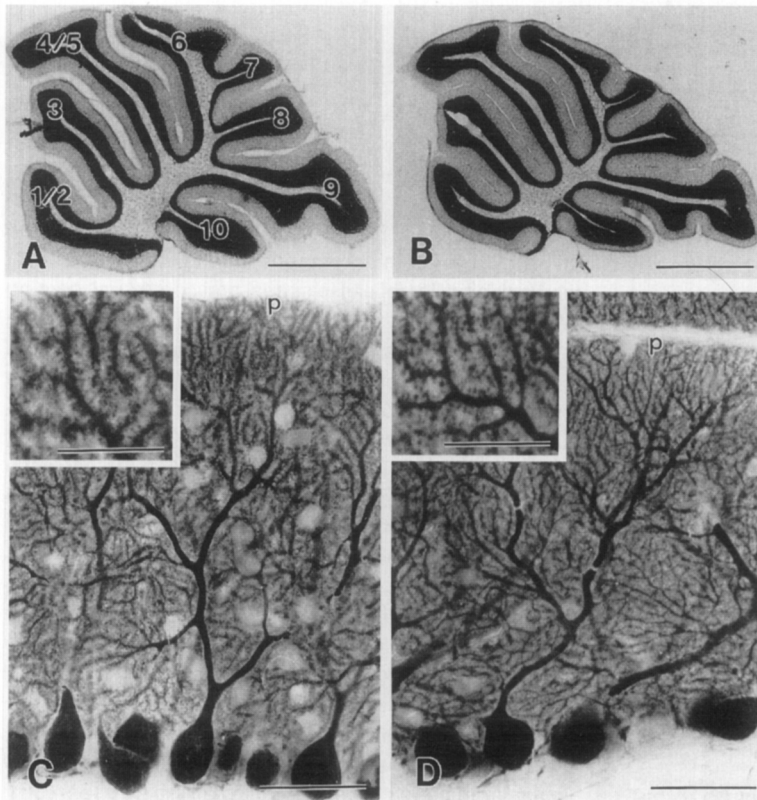


**Figure 1. Histological and Immunohistochemical Analyses of the PKC $\gamma$  Mutant and Wild-Type Cerebella**

(A and B) Toluidine blue-stained sagittal sections through the cerebellar vermis, from PKC $\gamma$  mutant (A) and wild-type (B) mice.

(C and D) Cerebellar cortex, from PKC $\gamma$  mutant (C) and wild-type (D) mice, immunostained for spot 35/calbindin.

The lobule number of the mouse cerebellum is indicated as 1–10, according to Marani and Voogd (1979). The rostral is to the left, and dorsal is to the top in (A) and (B). P, pia matter. Scale bars: (A) and (B), 1 mm; (C) and (D), 20  $\mu$ m; insets, 50  $\mu$ m.

## Results

### Morphology of PKC $\gamma$ Mutant Cerebellum

Cerebella of PKC $\gamma$  mutant mice appear morphologically indistinguishable from those of wild-type mice at the gross anatomical level. Histologically, the cerebella of the mutant mice exhibited well-developed foliation, comparable to that of the wild-type mice (Figures 1A and 1B). Laminar organization of the cerebellular cortex, including the granular cell, the PC, and molecular layers, is clearly discernible in PKC $\gamma$  mutant mice. Morphology of PCs was examined by immunohistochemistry with antibody against spot 35/calbindin, a cytosolic Ca<sup>2+</sup>-binding protein specific to PCs (Garcia-Segura et al., 1984; Yamakuni et al., 1984). In both mutant and wild-type mice, PCs align in monolayer between the granular and molecular layers, and well-differentiated dendritic arbors extend from the apical pole toward the pial surface (Figures 1C and 1D). In addition, numerous tiny punctations representing spines of the PCs were observed along the dendritic trees (insets in Figures 1C and 1D).

Synapses in the molecular layer were examined by electron microscopy. In both wild-type and mutant mice, the majority of these structures were asymmetric and consisted of presynaptic axonal terminals containing clear round vesicles and postsynaptic dendritic spines with marked postsynaptic density (Figure 2). These structures are typical of PF–PC synapses. When quantitated on electron micrographs, the number of synapses having these characteristics was  $22.0 \pm 0.9$  per 100  $\mu$ m<sup>2</sup> (mean  $\pm$  SEM,  $n = 10$ ),  $21.9 \pm 0.8$ , and  $18.1 \pm 0.8$  for three mutant

mice, and  $23.0 \pm 0.8$ ,  $22.8 \pm 1.1$ , and  $20.7 \pm 0.8$  for three wild-type mice, with no significant difference between the mutant and wild-type mice ( $p = 0.19$ ,  $t$  test). These observations suggest that the deletion of the PKC $\gamma$  gene did not affect gross development of the cerebellar anatomy, differentiation of the PC morphology, and the formation of the PF–PC synapses.

### Mutant PCs Are Multiply Innervated by CFs

In sagittal cerebellar slices prepared from 22- to 25-day-old (P22–P35) wild-type mice or age-matched mutant animals, CFs were stimulated in the granule cell layer and evoked responses in single PCs that were recorded using patch-clamp techniques in the whole-cell configuration (Konnerth et al., 1990; Llano et al., 1991; Kano et al., 1992). In all wild-type PCs but one, a large excitatory postsynaptic current (EPSC) was elicited in an all-or-none fashion as the stimulus intensity was gradually increased (pulse width 0.1 ms, strength 0–100 V) (Figure 3A). By contrast, in 41% (29 out of 71) of mutant PCs, CF-mediated EPSCs (CF-EPSCs) had two or three discrete steps when the stimulus intensity was above the threshold (Figure 3A). Frequency distribution of PCs in terms of number of CF-EPSC steps (Figure 3B, left) shows significant difference between the wild-type and mutant mice ( $p < 0.001$ ,  $\chi^2$  test). This indicates that, during P22–P35, most PCs in the wild-type mice are innervated by single CFs, while more than 40% of mutant PCs are innervated by multiple CFs.

This difference of CF innervation between wild-type and PKC $\gamma$  mutant mice during P22–P35 could be due to the retardation of general cerebellar maturation in the mutant

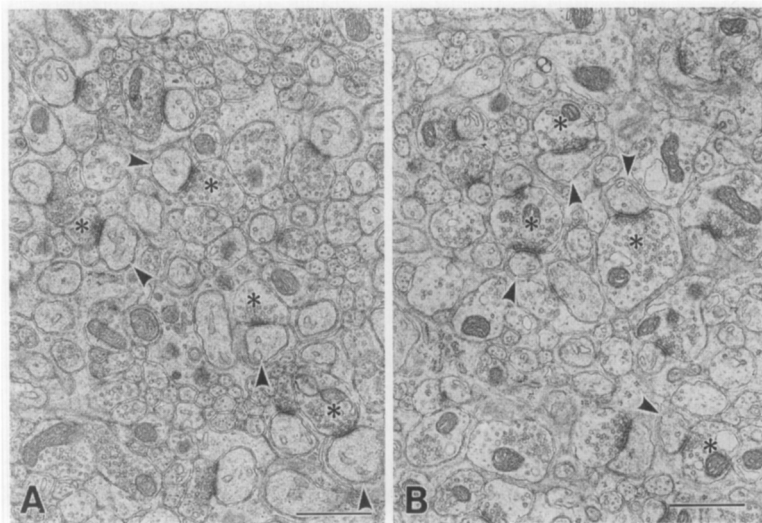


Figure 2. Electron Micrographs of the Molecular Layer of the PKC $\gamma$  Mutant and Wild-Type Cerebella

Cerebella are from PKC $\gamma$  mutant (A) and wild-type (B) mice. Asterisks indicate presynaptic terminals, while arrowheads indicate postsynaptic dendritic spines. Scale bar, 1  $\mu$ m.

mice. To assess this possibility, we examined CF-EPSCs in older mice (P50–P70) (Figure 3B, right). All but one wild-type PC had exclusively single CF responses, while 31% (10 out of 32) of mutant PCs had multiple steps. The distributions were significantly different between the wild-type and mutant mice ( $p < 0.001$ ,  $\chi^2$ ). Thus, substantial percentages of mutant PCs remain multiply innervated by CFs even in 7- to 10-week-old mice, suggesting that the notion of the retardation of general maturation is unlikely to be correct.

#### Kinetics, Short-Term Plasticity, and I-V Relations of CF-EPSCs Are Normal

To examine whether the kinetics of CF-EPSCs were altered in the mutant mice, we measured the 10%–90% rise time and the decay time constant of CF-EPSCs in the wild-type and mutant mice (Table 1). The decay time constants were obtained by fitting the decay phases of CF-EPSCs with single exponentials (Llano et al., 1991). The data from mutant mice were divided into two groups, those from mono-innervated PCs and those from multiply innervated PCs. In the latter group, measurements were done on the first step of multiple CF-EPSCs that appeared with the lowest stimulus intensity. Both the 10%–90% rise time and the decay time constant were similar among the three cell groups listed in Table 1. On the other hand, the average amplitudes of CF-EPSCs of the mutant multiply innervated PCs were less than 50% of the amplitudes of mono-innervated PCs taken from either mutant or wild-type mice when measured at a holding potential of  $-20$  mV (Table 1). The amplitudes of the latter two groups were not significantly different (Table 1). These results indicate that kinetics of CF-EPSCs in the mutant mice are normal.

Short-term historic effects, reflected as the response to the second stimulus of a pulse pair, are one important aspect of synaptic function. It has been reported that CF-EPSCs display a depression to the second stimulus of a pulse pair (Konnerth et al., 1990). In both mono-innervated and multiply innervated mutant PCs, CF-EPSCs showed prominent paired pulse depression (Figure 4A). During

both P22–P35 and P50–P70, the amplitudes of paired pulse depression were not significantly different from those of the mono-innervated PCs from the wild-type mice at all interpulse intervals tested (Figure 4). Thus, short-term synaptic plasticity is unimpaired at CF synapses in the mutant mice. Paired pulse synaptic plasticity is presumably caused by a change in transmitter release from presynaptic terminals (Zucker, 1989). Therefore, the present results suggest that presynaptic functions of CF terminals are unimpaired in the mutant mice.

During both P22–P35 and P50–P70, the current–voltage

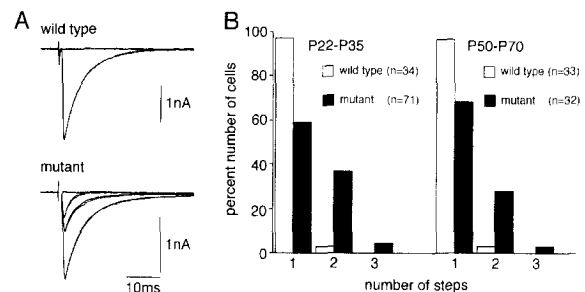


Figure 3. Multiple CF Innervation of PCs in Mature Mutant Mice

(A) EPSCs elicited by stimulation of CFs in the granule cell layer in a wild-type PC (P25) and a mutant (P23) PC. As the stimulus intensity was gradually increased, CF-EPSCs of the wild-type cell behaved in an all-or-none fashion, while those of the mutant cell had three discrete steps, indicating that at least three CFs innervate this mutant PC. Stimuli were applied at 0.1 Hz. Holding potential was  $-20$  mV for the wild-type PC and  $-30$  mV for the mutant cell.

(B) Summary histograms showing the number of discrete steps of CF-EPSCs of the wild-type (open columns) and mutant (stippled columns) PCs. Data obtained from mice at postnatal day 22–35 (P22–P35, left) and at P50–P70 (right), respectively. Note that nearly all wild-type PCs had only one step, while a substantial percentage of mutant PCs had more than two steps, at both P22–P35 (left) and at P50–P70 (right). Numbers of tested PCs at P22–P35 (left) are  $n = 34$  (from 6 wild-type mice, 19 cells studied blind to the mouse genotype) and  $n = 71$  (from 10 mutant mice, 34 cells studied blind). Those at P50–P70 (right) are  $n = 33$  (from 3 mice, 26 cells studied blind) and  $n = 32$  (from 3 mice, all cells studied blind).

Table 1. Kinetics of CF-EPSCs and PF-EPSCs

Genotype	10%–90% Rise Time (ms)	Decay Time Constant (ms)	Amplitude <sup>a</sup> (pA, V <sub>h</sub> = -20 mV)
<b>CF-EPSC</b>			
Wild type (mono)	0.5 ± 0.1 (n = 14)	6.7 ± 2.5 (n = 14)	1310 ± 555 (n = 8)
Mutant (mono)	0.5 ± 0.1 (n = 13)	6.8 ± 1.5 (n = 13)	1518 ± 470 (n = 7)
Mutant (multi) <sup>b</sup>	0.5 ± 0.1 (n = 13)	6.4 ± 3.5 (n = 13)	599 ± 310 (n = 11)
<b>PF-EPSC</b>			
Wild type	1.4 ± 0.3 (n = 16)	13.0 ± 2.9 (n = 16)	
Mutant	1.2 ± 0.2 (n = 15)	12.1 ± 3.1 (n = 15)	

All data are expressed as mean ± SD and sample size.

<sup>a</sup> Amplitudes of CF-EPSCs were measured at the holding potential (V<sub>h</sub>) of -20 mV.

<sup>b</sup> Only the first step of multiple CF-EPSPs was used for analysis.

age (I–V) relations of CF-EPSCs were linear in the wild-type monoinnervated (Figure 5A), the mutant monoinnervated (Figure 5B), and the mutant double-innervated (Figure 5C) PCs. It should be noted that, in the mutant double-innervated PCs, both the first and second steps of CF-EPSCs showed linear current–voltage relations and similar reversal potentials (Figure 5C). This indicates that EPSCs elicited by each of the two CFs are based on the

same ionic mechanism. Furthermore, CF-EPSCs in both the wild-type and mutant mice during P22–P35 were not affected by an N-methyl-D-aspartic acid (NMDA) blocker, DL-2-amino-5-phosphonopentanoate (AP5, 100 μM), but were totally suppressed by a non-NMDA antagonist, 6-cyano-7-nitroquinoxaline-2,3-dione (CNQX, 10 μM) (data not shown). These results indicate that CF-EPSCs of mature PCs from the wild-type and mutant mice are exclusively mediated by non-NMDA subtypes of glutamate receptors.

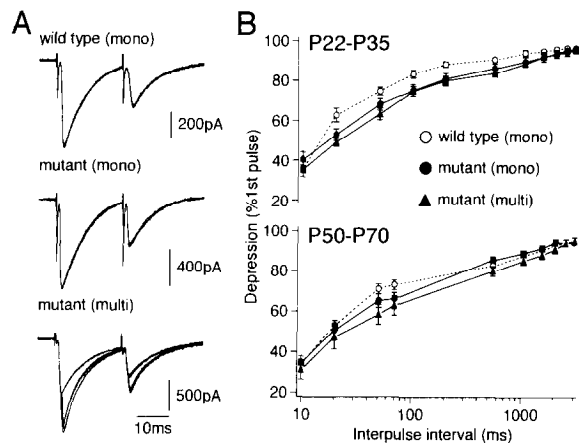


Figure 4. CF-EPSCs Display Normal Short-Term Synaptic Plasticity in the Mutant PCs

(A) CF-EPSCs to pairs of stimuli separated by 20 ms in a wild-type monoinnervated PC (top, P25), a mutant monoinnervated PC (middle, P25), and a mutant double-innervated PC (bottom, P25). Three to five traces were superimposed. Note that the responses to the second stimuli were markedly depressed in all traces. Stimulus pairs were applied at 0.1 Hz. Holding potential was -20 mV, except for the cell in the bottom panel (-30 mV).

(B) Summary graphs showing paired-pulse depression of CF-EPSCs in the wild-type monoinnervated (open circles), mutant monoinnervated (closed circles), and mutant multiply innervated (closed triangles) PCs from mice at P22–P35 (top) and P50–P70 (bottom). The second response (expressed as percentage of response to the first pulse, mean ± SEM) is plotted as a function of interpulse intervals. Stimulus pairs were applied at 0.1 Hz. Numbers of tested PCs at P22–P35 (top) are n = 13 (from 6 mice, 6 cells studied blind) for the wild-type (mono), n = 14 (from 7 mice, 4 cells studied blind) for the mutant (mono), and n = 21 (from 7 mice, 9 cells studied blind) for the mutant (multi). Those at P50–P70 (bottom) are n = 9 (from 3 mice) for the wild-type (mono), n = 12 (from 4 mice) for the mutant (mono), and n = 9 (from 3 mice) for the mutant (multi). All cells were studied blind to the mouse genotype for the data at P50–P70.

### CF Innervation during Early Postnatal Days

These results indicate that adult PKC $\gamma$  mutant mice exhibit normal presynaptic function and postsynaptic receptor pharmacology at CF–PC synapses. In contrast, innerva-

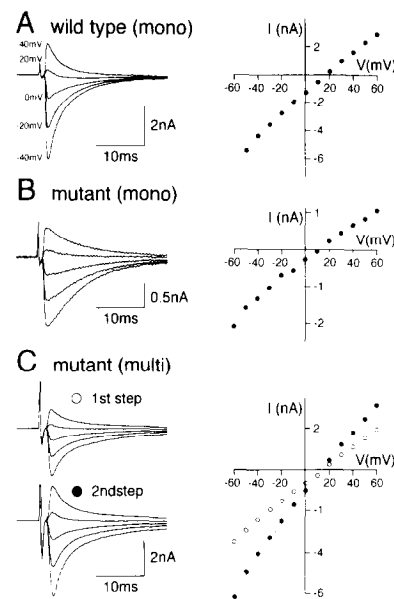
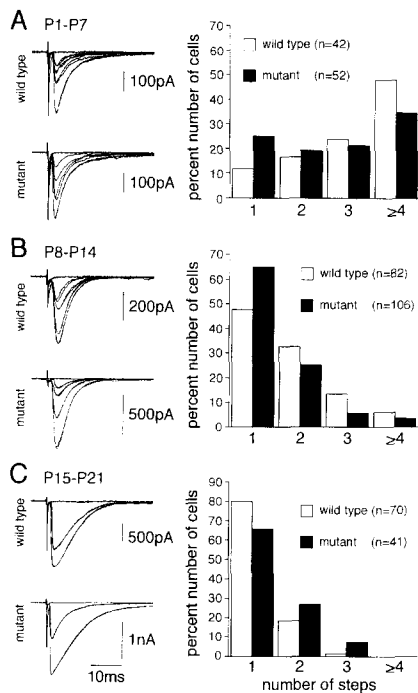


Figure 5. Current–Voltage Relations of CF-EPSCs Are Normal in PKC $\gamma$  Mutant Mice

Single CF-EPSCs recorded at holding potentials of -40 mV, -20 mV, 0 mV, 20 mV, and 40 mV (left) and corresponding current–voltage relations of CF-EPSCs (right) in a wild-type monoinnervated PC (A, P25), a mutant monoinnervated PC (B, P25), and a mutant double-innervated PC (C, P70).



**Figure 6. Early Postnatal Development of CF Innervation**  
(A, left) CF-EPSCs of the wild-type (P1, holding potential  $-60$  mV) and mutant (P1, holding potential  $-60$  mV) PCs. One to three traces each were superimposed at threshold intensities. Stimuli were applied at  $0.1$  Hz.  
(A, right) Summary graph showing numbers of multiple steps of CF-EPSCs of the wild-type (open columns) and mutant (stippled columns) PCs from mice at P1–P7. Numbers of tested PCs are  $n = 42$  (from 8 wild-type mice, 7 cells studied blind) and  $n = 52$  (from 10 mutant mice, 14 cells studied blind).  
(B) Similar to (A), but examples of CF-EPSCs of the wild-type (P12, holding potential  $-10$  mV) and mutant (P8, holding potential  $-60$  mV) PCs and summary graph of the data from mice at P8–P14. Numbers of tested PCs are  $n = 82$  (from 13 wild-type mice, 30 cells studied blind) and  $n = 106$  (from 17 mutant mice, 44 cells studied blind).  
(C) Similar to (A) and (B), but examples of CF-EPSCs of the wild-type (P17, holding potential  $-20$  mV) and mutant (P15, holding potential  $-30$  mV) PCs and summary graph of the data from mice at P15–P21. Numbers of tested PCs are  $n = 70$  (from 5 mice, 11 cells studied blind) and  $n = 41$  (from 4 mice, 31 cells studied blind).

tion of PCs by CFs is abnormal in that a substantial percentage (41%) of PCs continues to be innervated by multiple CFs in adult mice. This abnormality may arise from either augmented CF innervation during early postnatal days or impaired CF elimination in a subsequent period, or both. To examine these possibilities, we followed the developmental course of CF innervation during the first three postnatal weeks.

We observed that during the first postnatal week (P1–P7), the majority of PCs were multiply innervated by CFs in both wild-type and mutant mice (Figure 6A). In particular, more than one-third of PCs were innervated by more than four CFs in both strains of mice. However, the frequency distribution of the number of CF-EPSC steps per PC in the mutant mice was not significantly different from that in the wild-type mice ( $p > 0.05$ ,  $\chi^2$  test).

During the second postnatal week (P8–P14), the per-

centage of PCs with multiple CF-EPSC steps decreased markedly in both wild-type and mutant mice (Figure 6B), although about 50% of PCs were still multiply innervated in each strain. The difference between the frequency distributions of PCs during P1–P7 and those during P8–P14 were highly significant for both the wild-type and mutant mice ( $p < 0.001$ ,  $\chi^2$  test). On the other hand, the distributions were not significantly different between the two strains during P8–P14 ( $p > 0.05$ ,  $\chi^2$  test).

During the third postnatal week (P15–P21), the percentage of PCs with multiple CF-EPSC steps further decreased in the wild-type mice (Figure 6C). In contrast, no further decrease was observed during the same period in mutant mice (Figure 6C). When the data in Figure 6 are compared with those in Figure 3, we notice that the average percentage of PCs with multiple CF-EPSC steps further decreased from the third postnatal week (P14–P21) to the fourth postnatal week ( $p < 0.01$ ,  $\chi^2$  test). The data suggest that the adult pattern of monoinnervation is not established until the end of the third postnatal week. In the mutant mice, the percentage of PCs with multiple CF-EPSC steps during the fourth postnatal week remains at the level (about 40%) reached during the previous week ( $p > 0.05$ ,  $\chi^2$  test).

These results indicate that CF innervation of the mutant mice during early postnatal days (P1–P14) appears normal. In the wild-type mice, progressive decrease of the percentage of multiply innervated PCs continues during P15–P21, while this process appears to be lacking in the mutant mice. These results suggest that synapse elimination process that occurs during the third postnatal week is specifically impaired in the mutant mice. Thus, in terms of CF–PC connections, mutant cerebella seem to remain immature throughout adult life, namely at the stage of the second postnatal week.

#### NMDA Receptors Are Not Involved in CF-EPSCs of Immature Mice

A previous study showed that the elimination of supernumerary CFs during cerebellar development requires activation of NMDA receptors in the cerebellum (Rabacchi et al., 1992). However, it is unclear whether NMDA receptors on PCs or those on other types of cells are involved in this process. Thus, we examined the effects of AP5 ( $100 \mu\text{M}$ ) on CF-EPSCs in both monoinnervated and multiply innervated PCs that were sampled in immature wild-type (Figure 7A) and mutant (Figure 7B) mice. CF-EPSCs were little affected by AP5 in any of these cases, but were totally suppressed by CNQX ( $10 \mu\text{M}$ ) (Figures 7A and 7B), demonstrating that CF-EPSCs in the immature wild-type and mutant mice are mediated exclusively by non-NMDA receptors. Thus, although NMDA receptor activation appears to be required for the elimination of supernumerary CFs during cerebellar development (Rabacchi et al., 1992), CF–PC transmission is not involved in this process.

#### PF-Mediated EPSCs Are Normal

The nature of EPSCs elicited by stimulation of PFs, the other major excitatory input to PCs, was examined in trans-

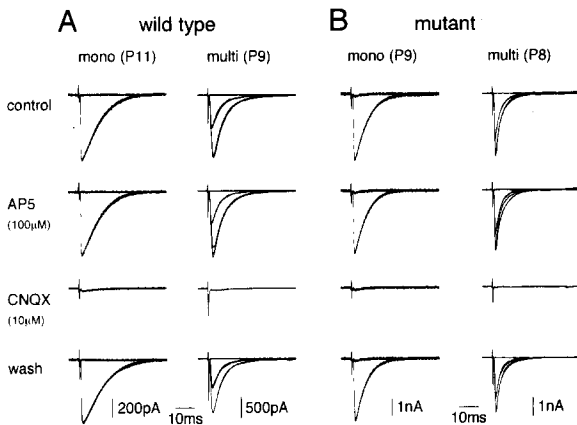


Figure 7. Pharmacology of CF-EPSCs in Immature PCs

(A) CF-EPSCs of a mono-innervated wild-type PC (left, P11, holding potential 0 mV) and a double-innervated wild-type PC (right, P9, holding potential -60 mV).

(B) CF-EPSCs of a mono-innervated mutant PC (left, P9, holding potential -20 mV) and a double-innervated mutant PC (right, P8, holding potential -60 mV).

Note that, in all of the cells, CF-EPSCs were little affected by a specific NMDA receptor antagonist, AP5 (100 μM), but were totally blocked by a non-NMDA receptor antagonist, CNQX (10 μM). In all records, the perfusate was Mg<sup>2+</sup>-free Ringer containing 10 μM glycine to maximize NMDA receptor-mediated currents. AP5 and CNQX were bath applied. Stimuli were repeated at 0.1 Hz. Three to five traces each were superimposed at threshold intensities. Holding potential was -60 mV, except for the mutant in (B) (-70 mV).

verse cerebellar slices from mice at P18–P26. In both wild-type and mutant PCs, PF-EPSCs were little affected by AP5 (100 μM), but were totally suppressed by CNQX (10 μM) (Figure 8A). These results confirm that both CF-EPSCs and PF-EPSCs in PCs are mediated exclusively by non-NMDA receptors (Llano et al., 1991).

PF-EPSCs of both wild-type and mutant PCs displayed prominent facilitation to the second of a stimulus pair (Figure 8B), as previously reported (Konnerth et al., 1990; Aiba et al., 1994). The amplitudes of paired pulse facilitation in the mutant mice (Figure 8B, closed circles) were not significantly different from those of the wild-type mice (Figure 8B, open circles) at all interpulse intervals tested. Thus, presynaptic functions of PF terminals appear to be unimpaired in the mutant mice.

## Discussion

### Persistent Multiple CF Innervation in PKC $\gamma$ Mutant Mice

The present study demonstrates that multiple CF innervation persists in a substantial percentage of cerebellar PCs in PKC $\gamma$  mutant mice. On the other hand, CF-EPSCs appear normal in many aspects, such as paired pulse depression (Figure 4), current–voltage relations (Figure 5), time course, and pharmacology (Table 1). These results indicate that properties of the presynaptic terminal and the postsynaptic membrane of CF–PC synapses are normal in the mutant mice.

Regression of multiple CF innervation appears to prog-

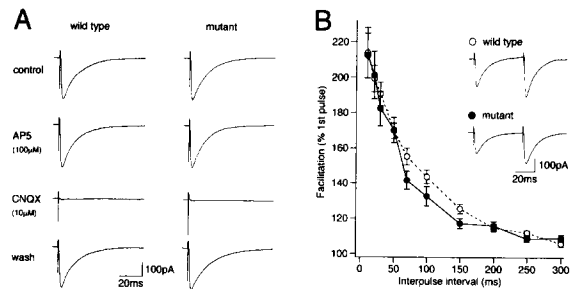


Figure 8. PF-EPSCs Are Normal in the Mutant PCs

(A) PF-EPSCs of a wild-type PC (left, P23) and a mutant PC (right, P26). Note that PF-EPSCs were little affected by AP5 (100 μM), but were totally suppressed by CNQX (10 μM). The perfusate was Mg<sup>2+</sup>-free Ringer containing 10 μM glycine, and AP5 and CNQX were bath applied. Stimuli were repeated at 1 Hz. Each trace is the average of ten consecutive EPSCs. Holding potential was -60 mV.

(B) Paired-pulse facilitation of PF-EPSCs in the wild-type (open circles, n = 11 from 10 mice, 3 cells studied blind) and mutant (closed circles, n = 8 from 6 mice, 6 cells studied blind) PCs. The second response (expressed as percentage of response to the first pulse, mean ± SEM) is plotted as a function of interpulse intervals. Stimulus pairs were applied at 1 Hz. Insets show example of PF-EPSCs to pairs of stimuli separated by 50 ms in transverse cerebellar slices from wild-type (P25) and mutant (P21) mice. Each trace is the average of ten consecutive EPSCs. Holding potential was -60 mV.

ress in at least two distinct steps. In the rat and probably also in the mouse, dendrites of PCs have not yet developed by the end of the first postnatal week. At this timepoint, a hypertrophied apical cone and lateral processes are seen around the soma, and the latter structure is contacted by multiple CFs (Altman, 1972). Within the first few days of the second postnatal week, the dendrites grow, and as they appear, the somatic processes and the CF synapses onto them start to disappear. This is the first step of the regression of CF innervation. The CFs are then displaced upward to form synaptic contacts on the growing dendrites (O'Leary et al., 1971; Palay and Chan-Palay, 1974). During the second 10 days of the postnatal life, the dendritic tree of PCs develops dramatically, and PFs form synaptic contacts on dendritic spines. The number of synaptic contacts from CFs on the dendrites increases and, in a coordinated fashion, the number of CFs innervating each PC continues to decrease. This is the second step of the regression of CF innervation.

Our results indicate that regression of multiple CF innervation occurs normally in the PKC $\gamma$  mutant mice during the second postnatal week, but is greatly diminished thereafter. This suggests that the first and second steps of the regression of CF innervation is mediated by different mechanisms and that PKC $\gamma$  is critically involved only in the second step. This latter suggestion is consistent with the observation that PKC $\gamma$  expression in the cerebellum reaches a maximal level during the third postnatal week (Yoshida et al., 1988; Huang et al., 1990; Nishizuka, 1988).

### Comparison with Other Mutants with Multiple CF Innervation

It was previously reported that multiple CF innervation persists in the cerebella of adult animals that are devoid of

granule cells during early postnatal development (Crepel, 1982). Previous animal models include rats in which granule cells have been destroyed by X-irradiation (Woodward et al., 1974; Crepel and Delhaye-Bouchaud, 1979), weaver mutant mice in which granule cells die during their migration (Crepel and Mariani, 1976), and reeler mice in which some PCs are devoid of synaptic contacts with granule cells (Mariani et al., 1977). The multiple innervation also persists in staggerer mutant mice, in which granule cells develop normally, but then degenerate without making synaptic contacts with PCs (Crepel et al., 1980; Mariani and Changeux, 1980). Thus, the presence of granule cells and PF-PC synaptogenesis appear to be essential for the regression of multiple CF innervation of PCs.

Recently, multiple CF innervation of PCs was reported in mutant mice deficient in  $\delta 2$  subunit of glutamate receptors (GluR $\delta 2$ ) (Kashiwabuchi et al., 1995). In GluR $\delta 2$  mutant mice, the gross morphology of the cerebellum appears normal, and PCs appear to develop normally with well-branched dendrites and spines. Moreover, PF-PC transmission is functional. However, inspection by electron microscopy showed that the number of synaptic contacts from PFs onto dendritic spines of PCs are less than half of that of wild-type mice (Kashiwabuchi et al., 1995). Thus, it is likely that the observed multiple innervation in the GluR $\delta 2$  mutant mice is a result of insufficient PF inputs, consistent with the earlier mutant studies. In addition, GluR $\delta 2$  may also have an effect on CF elimination that does not involve PF inputs. In contrast with these previously described mutants, the PKC $\gamma$  mutant mice exhibit no abnormalities in PF-PC synapses that are detectable with morphological or electrophysiological methods.

#### **Role of PKC $\gamma$ in the Elimination of Multiple CF Innervation**

There is substantial data indicating that, within the cerebellum, PKC $\gamma$  expression is limited to PCs (Huang et al., 1990; Ase et al., 1988; Hidaka et al., 1988; Kose et al., 1988; Kitano et al., 1987; Brandt et al., 1987). Huang et al. (1990) demonstrate that throughout postnatal cerebellar development, PKC $\gamma$  is present only in PCs and not in granule cells or other cell types. Linden et al. (1992) recapitulate this result in cerebellar neuronal cultures. There is one report claiming that PKC $\gamma$  mRNA is detectable in granule cells of the developing cerebellum (Herms et al., 1993). However, it is not clear how specific the hybridization probe was for PKC $\gamma$  in this study. We recently reexamined this issue using a different hybridization probe whose specificity for the PKC $\gamma$  isoform was demonstrated. We confirmed that PKC $\gamma$  mRNA is restricted to PCs in the developing cerebellum (our unpublished data).

There is also evidence that PKC $\gamma$  is absent from the inferior olive, where CFs originate. No PKC $\gamma$  mRNA is observed in the inferior olive of adult rats (Brandt et al., 1987). We recently observed similar results with postnatal day 21 rats (our unpublished data). Furthermore, PKC $\gamma$  protein is undetectable in the rat medulla oblongata, where the inferior olive is situated (Huang et al., 1987).

We propose that the deficiency in the elimination of multiple CF innervation in PKC $\gamma$  mutant mice is due to the

lack of this kinase in PCs. This proposal is based on the observations that no physiological or anatomical alternations are detectable in PC or CF pathways of PKC $\gamma$  mutant mice, and the expression of PKC $\gamma$  is limited to PCs among the neurons that participate in these pathways. We cannot exclude the possibility that PKC $\gamma$  deficiency elsewhere, such as in the cerebral cortex or hippocampus, leads indirectly to deficient CF synapse elimination. However, there is no evidence that suggests the participation of these structures in the elimination of multiple CF innervation. We also cannot exclude the possibility that PKC $\gamma$  expressed at levels below the detection limit is crucially involved in CF elimination. To address this point, we intend to generate mutant mice in which PKC $\gamma$  is deficient uniquely in PCs.

If PKC $\gamma$  in PCs is crucially involved in the elimination of multiple CF innervation, what is its role? PCs are physiologically and anatomically unaltered in the PKC $\gamma$  mutant mice, so it is unlikely that the PKC $\gamma$  deficiency leads to a pleiotropic defect in PCs. Previous data from other mutant mice (see above) have suggested that PF-PC synapses are required for CF synapse elimination. We propose that activity in the PF-PC pathway signals the elimination of multiple CF innervation in an activity-dependent, heterosynaptic fashion. We suggest that PKC $\gamma$  transduces this signal. It has been hypothesized that the elimination of CF innervation results from competitive multiple interactions among CFs for a limiting factor (Crepel, 1982), such as a neurotrophic factor, and that PF-PC activity fuels this competition. Perhaps, PKC $\gamma$  is in one or both of the biochemical cascades that reside downstream of the PF-PC or CF-PC (or both) activities.

In one study, NMDA receptors have been implicated in the regression of multiple CF innervation. Rabacchi et al. (1992) reported that multiple innervation persists to a significant extent in rats chronically treated with the NMDA receptor antagonist AP5. The authors suggest that NMDA receptors, present on PCs, granule cells, or both, are involved in the elimination of multiple CF innervation. Transient expression of NMDA receptors on developing PCs is controversial (Watanabe et al., 1994; Akazawa et al., 1994). Furthermore, we do not observe an NMDA receptor component to either PF-EPSCs or CF-EPSCs in immature cerebellum, as might be expected if NMDA receptors in PCs played a role in synapse elimination. In contrast, expression of NMDA receptors is well established in granule cells (Watanabe et al., 1994; Akazawa et al., 1994). Therefore, if NMDA receptors play a role in the elimination of multiple CF innervation, it may be through an indirect mechanism involving granule cells. This is consistent with the aforementioned data linking synapse elimination to the presence of granule cells or the formation of PF-PC synapses.

#### **Experimental Procedures**

##### **Production of PKC $\gamma$ Mutant Mice**

PKC $\gamma$  mutant mice were produced as described previously (Abeliovich et al., 1993a). Both wild-type and mutant mice utilized were of 129/Sv  $\times$  C57BL/6 genetic background and were kept in the same room, at the animal facility of the Massachusetts Institute of Technology, with a 12 hr light-dark cycle.

### Histology

Under deep anesthesia with chloral hydrate (350 mg/kg body weight, intraperitoneally), mice at the fifth postnatal week were perfused from the left ventricle of the heart with freshly prepared 4% paraformaldehyde in 0.1 M sodium phosphate buffer (pH 7.2). The brain was quickly removed from the skull and immersed in the same fixative overnight. Parasagittal brain sections of 50 and 100  $\mu\text{m}$  in thickness were prepared by a Cryostat (Bright) or by a microslicer (Dosaka), respectively. Cryostat sections mounted on gelatin-coated slides were Nissl-stained with toluidine blue. Microslicer sections were immunostained with rabbit anti-rat spot 35/calbindin antibody (Yamakuni et al., 1984). Following visualization with ABC kit (Vector Labs), the sections were treated with 0.5%  $\text{OsO}_4$  for 15 min to enhance the immunostaining.

### Electron Microscopy and Morphometry

For electron microscopy, mice in the fifth postnatal week were perfused from the heart with 0.5% glutaraldehyde and 4% paraformaldehyde in 0.1 M sodium cacodylate buffer (pH 7.2). After sectioning at a thickness of 400  $\mu\text{m}$  by a microslicer in the parasagittal plane, sections through the midline of the cerebellum were chosen and immersed in the same fixative for 4–6 hr. The sections were postfixed for 2 hr with 1%  $\text{OsO}_4$  in 0.1 M sodium cacodylate buffer (pH 7.2), dehydrated using graded alcohols, and embedded in Epon 812. Silver-gold ultrathin sections through the culmen (lobule 4+5) were collected on copper grids and stained with 1% uranyl acetate for 5 min and mixed with lead solution for 2 min.

From each mouse, ten sets of electron micrographs were prepared, each set being composed of 6–15 micrographs taken serially from the deepest region of the molecular layer up to the pial surface, at an original magnification of 3,000 $\times$  with a Hitachi H7100 electron microscope. For quantitative measurements, the number of synaptic profiles was counted for each set of electron micrographs printed at a final magnification of 11,400 $\times$ . The counted neuropil area, which excludes vessels, cell bodies, and dendritic shaft thicker than 2  $\mu\text{m}$  in caliber, was measured by the point-counting method of Weibel (1979), using the double lattice system. The mean synaptic number per 100  $\mu\text{m}^2$  was calculated for each mouse from the synaptic number and the counted neuropil area.

### Electrophysiology

Cerebellar slices were prepared from the wild-type and mutant mice as described previously (Edwards et al., 1989; Llano et al., 1991; Kano and Konnerth, 1992; Aiba et al., 1994). Cerebellar slices of 200–300  $\mu\text{m}$  thickness were cut with a vibraslicer (Campden) and kept at 32°C for at least 1 hr in a chamber containing standard saline (see below) that was bubbled with 95%  $\text{O}_2$  and 5%  $\text{CO}_2$ . One slice was then transferred to a recording chamber where it was continuously perfused with the oxygenated standard saline. Recognition of layers within the cerebellar cortex and identification of PCs were easily achieved on slices when viewed using a 40 $\times$  water immersion objective attached to a Zeiss upright microscope (Axioscope) (Edwards et al., 1989; Llano et al., 1991). All experiments were performed using whole-cell configuration of the patch-clamp technique with borosilicate pipettes (resistance of 3–6 M $\Omega$  when filled with an intracellular solution; see below). Ionic currents were recorded with an EPC-9 patch-clamp amplifier (HEKA) and stored on a DAT data recorder (Sony, PC204) for later analysis. The pipette access resistance was compensated as explained by Llano et al. (1991). Stimulation and on-line data acquisition were performed using the PULSE program on a Macintosh computer (version 7.5, HEKA). The signals were filtered at 3 kHz and digitized at 20 kHz. Fitting of the decay phases of EPSCs was done with the PULSE-FIT program (version 7.5, HEKA). For stimulation of CFs and PFs, a glass pipette with 5–10  $\mu\text{m}$  tip diameter filled with standard saline was used. Square pulses (duration, 0.1 ms; amplitude, 0–100 V for CF stimulation, 1–10 V for PF stimulation) were applied for focal stimulation.

The composition of standard saline was 125 mM NaCl, 2.5 mM KCl, 2 mM  $\text{CaCl}_2$ , 1 mM  $\text{MgSO}_4$ , 1.25 mM  $\text{NaH}_2\text{PO}_4$ , 26 mM  $\text{NaHCO}_3$ , and 20 mM glucose, which was bubbled continuously with a mixture of 95%  $\text{O}_2$  and 5%  $\text{CO}_2$ . Bicuculline (10 mM) was always present in the saline to block spontaneous inhibitory postsynaptic currents (Konnerth et al. 1990; Kano et al., 1992). The standard pipette solution contained 60  $\mu\text{M}$  CsCl, 30  $\mu\text{M}$  Cs D-gluconate, 20  $\mu\text{M}$  BAPTA, 4  $\mu\text{M}$   $\text{MgCl}_2$ , 4

$\mu\text{M}$  ATP, and 30  $\mu\text{M}$  HEPES (pH 7.3, adjusted with CsOH). In experiments for measuring PF-EPSCs, a K-based pipette solution was used (30 mM KCl, 90 mM K D-gluconate, 4 mM  $\text{MgCl}_2$ , 4 mM Na-ATP, 0.4 mM Na-GTP, and 50 mM HEPES [pH 7.3, adjusted with KOH]). All experiments were carried out at a bath temperature of 32°C.

### Acknowledgments

We thank K. Poss for reading the manuscript. This work was supported by the Howard Hughes Medical Institute (C. C., A. Aiba, and S. T.), National Institutes of Health grant RO1 NS32925 (S. T.), grants from the Japanese Ministry of Education, Science, and Culture (05454677, 06253216, and 06260237) (M. K.), the Uehara Foundation (M. K.), the Ciba-Geigy Foundation for the Promotion of Science (M. K.), and the Kato Memorial Bioscience Foundation (M. K.).

Received October 12, 1995; revised November 19, 1995.

### References

- Abeliovich, A., Chen, C., Goda, Y., Silva, A.J., Stevens, C.F., and Tonegawa, S. (1993a). Modified hippocampal long-term potentiation in PKC $\gamma$  mutant mice. *Cell* 75, 1253–1262.
- Abeliovich, A., Paylor, R., Chen, C., Kim, J.J., Wehner, J.M., and Tonegawa, S. (1993b). PKC $\gamma$  mutant mice exhibit mild deficits in spatial and contextual learning. *Cell* 75, 1263–1271.
- Aiba, A., Kano, M., Chen, C., Stanton, M.E., Fox, G.D., Herrup, K., Zwingman, T.A., and Tonegawa, S. (1994). Deficient cerebellar long-term depression and impaired motor learning in mGluR1 mutant mice. *Cell* 79, 377–388.
- Akazawa, C., Shigemoto, R., Bessho, Y., Nakanishi, S., and Mizuno, N. (1994). Differential expression of five N-methyl-aspartate receptor subunit mRNAs in the cerebellum of developing and adult rats. *J. Comp. Neurol.* 347, 150–160.
- Altman, J. (1972). Postnatal development of the cerebellar cortex in the rat. I. The external germinal layer and the transitional molecular layer. *J. Comp. Neurol.* 145, 353–398.
- Ase, K., Saito, N., Shearman, M.S., Kikkawa, U., Ono, Y., Igarashi, K., Tanaka, C., and Nishizuka, Y. (1988). Distinct cellular expression of  $\beta$ - and  $\beta$ II-subspecies of protein kinase C in rat cerebellum. *J. Neurosci.* 8, 3850–3856.
- Brandt, S.J., Niedel, J.E., Bell, R.M., and Young, W.S. (1987). Distinct patterns of expression of different protein kinase C mRNAs in rat tissues. *Cell* 49, 57–63.
- Chen, C., Kano, M., Abeliovich, A., Chen, L., Bao, S., Kim, J.J., Hashimoto, K., Thompson, R.F., and Tonegawa, S. (1995). Impaired motor coordination correlates with persistent multiple climbing fiber innervation in PKC $\gamma$  mutant mice. *Cell* 83, this issue.
- Crepel, F. (1982). Regression of functional synapses in the immature mammalian cerebellum. *Trends Neurosci.* 5, 266–269.
- Crepel, F., and Delhay-Bouchaud, N. (1979). Distribution of climbing fibers on cerebellar Purkinje cells in X-irradiated rats: an electrophysiological study. *J. Physiol.* 290, 97–112.
- Crepel, F., and Jaillard, D. (1991). Pairing of pre- and postsynaptic activities in cerebellar Purkinje cells induces long-term changes in synaptic efficacy: an *in vitro* study. *J. Physiol.* 432, 123–141.
- Crepel, F., and Krupa, M. (1988). Activation of protein kinase C induces a long-term depression of glutamate sensitivity of cerebellar Purkinje cells: an *in vitro* study. *Brain Res.* 458, 397–401.
- Crepel, F., and Mariani, J. (1976). Multiple innervation of Purkinje cells by climbing fibers in the cerebellum of the *weaver* mutant mouse. *J. Neurobiol.* 7, 579–582.
- Crepel, F., Delhay-Bouchaud, N., Gustavino, J.M., and Sampaio, I. (1980). Multiple innervation of cerebellar Purkinje cells by climbing fibres in *staggerer* mutant mouse. *Nature* 283, 483–484.
- Edwards, F.A., Konnerth, A., Sakmann, B., and Takahashi, T. (1989). A thin slice preparation for patch-clamp recordings from neurons of the mammalian central nervous system. *Pflügers Arch.* 414, 600–612.
- Garcia-Segura, L.M., Baetens, D., Roth, J., Norman, A.W., and Orci, L. (1984). Immunohistochemical mapping of calcium-binding protein

- immunoreactivity in the rat central nervous system. *Brain Res.* 296, 75–86.
- Harris, R.A., McQuilkin, S.J., Paylor, R., Abeliovich, A., Tonegawa, S., and Wehner, J.M. (1995). Mutant mice lacking the  $\gamma$  isoform of protein kinase C show decreased behavioral actions of ethanol and altered function of  $\gamma$ -aminobutyrate type A receptors. *Proc. Natl. Acad. Sci. USA* 92, 3658–3662.
- Hashimoto, T., Ase, K., Sawamura, S., Kikkawa, U., Saito, N., Tanaka, C., and Nishizuka, Y. (1988). Postnatal development of a brain-specific subspecies of protein kinase C in rat. *J. Neurosci.* 8, 1678–1683.
- Hemart, N., Daniel, H., Jaillard, D., and Crepel, F. (1995). Receptors and second messengers involved in long-term depression in rat cerebellar slices *in vitro*: a reappraisal. *Eur. J. Neurosci.* 7, 45–53.
- Hermes, J., Zurmohle, U., Schlingensiefen, K.-H., and Brysch, W. (1993). Transient expression of PKC $\gamma$  mRNA in cerebellar granule cells during rat brain development. *Neuroreport* 4, 899–902.
- Hidaka, H., Tanaka, T., Onoda, K., Hagiwara, M., Watanabe, M., Ohta, H., Ito, Y., Tsurudome, M., and Yoshida, T. (1988). Cell type-specific expression of protein kinase C isozymes in the rabbit cerebellum. *J. Biol. Chem.* 263, 4523–4526.
- Huang, F.L., Yoshida, Y., Nakabayashi, H., and Huang, K.-P. (1987). Differential distribution of protein kinase C isozymes in the various regions of brain. *J. Biochem. Chem.* 262, 15714–15720.
- Huang, F.L., Yoshida, Y., Nakabayashi, H., Young, W.S., and Huang, K.-P. (1988). Immunocytochemical localization of protein kinase C isozymes in rat brain. *J. Neurosci.* 8, 4734–4744.
- Huang, F.L., Young, W.S., Yoshida, Y., and Huang, K.-P. (1990). Developmental expression of protein kinase C isozymes in rat cerebellum. *Dev. Brain Res.* 52, 121–130.
- Ito, M. (1984). *The Cerebellum and Neural Control* (New York: Raven Press).
- Kano, M., and Konnerth, A. (1992). Cerebellar slices for patch clamp recording. In *Practical Electrophysiological Methods*, H. Kettenmann and R. Grantyn, eds. (New York: Wiley-Liss), pp. 54–57.
- Kano, M., Rexhausen, U., Dreessen, J., and Konnerth, A. (1992). Synaptic excitation produces a long-lasting rebound potentiation of inhibitory synaptic signals in cerebellar Purkinje cells. *Nature* 356, 601–604.
- Kashiwabuchi, N., Ikeda, K., Araki, K., Hirano, T., Shibuki, K., Takayama, C., Inoue, Y., Kutsuwada, T., Yagi, T., Kang, Y., Aizawa, S., and Mishina, M. (1995). Impairment of motor coordination, Purkinje cell synapse formation, and cerebellar long-term depression in GluR $\delta$ 2 mutant mice. *Cell* 81, 245–252.
- Kitano, T., Hashimoto, T., Kikkawa, U., Ase, K., Saito, N., Tanaka, C., Ichimori, Y., Tsukamoto, K., and Nishizuka, Y. (1987). Monoclonal antibodies against rat brain protein kinase C and their application to immunocytochemistry in nervous tissues. *J. Neurosci.* 7, 1520–1525.
- Konnerth, A., Llano, I., and Armstrong, C.M. (1990). Synaptic currents in cerebellar Purkinje cells. *Proc. Natl. Acad. Sci. USA* 87, 2662–2665.
- Kose, A., Saito, N., Ito, H., Kikkawa, U., Nishizuka, Y., and Tanaka, C. (1988). Electron microscopic localization of type I protein kinase C in rat Purkinje cells. *J. Neurosci.* 8, 4262–4268.
- Linden, D.J. (1994). Long-term synaptic depression in the mammalian brain. *Neuron* 12, 457–472.
- Linden, D.J., and Connor, J.A. (1991). Participation of postsynaptic PKC in cerebellar long-term depression in culture. *Science* 254, 1656–1659.
- Linden, D.J., Smeyne, M., Sun, S.C., and Conner, J.A. (1992). An electrophysiological correlate of protein kinase C isozyme distribution in cultured cerebellar neurons. *J. Neurosci.* 12, 3601–3608.
- Llano, I., Marty, A., Armstrong, C.M., and Konnerth, A. (1991). Synaptic- and agonist-induced excitatory currents of Purkinje cells in rat cerebellar slices. *J. Physiol.* 434, 183–213.
- Marani, E., and Voogd, J. (1979). The morphology of the mouse cerebellum. *Acta Morphol. Neerl. Scand.* 17, 33–52.
- Mariani, J., and Changeux, J.P. (1980). Multiple innervation of Purkinje cells by climbing fibers in the cerebellum of the adult *staggerer* mutant mouse. *J. Neurobiol.* 11, 41–50.
- Mariani, J., Crepel, F., Mikoshiba, K., Changeux, J.P., and Sotelo, C. (1977). Anatomical, physiological and biochemical studies of the cerebellum from *reeler* mutant mouse. *Phil. Trans. Roy. Soc. (Lond.) B* 287, 1–28.
- Moriya, M., and Tanaka, S. (1994). Prominent expression of protein kinase C ( $\gamma$ ) mRNA in the dendrite-rich neuropil of mice cerebellum at the critical period for synaptogenesis. *Neuroreport* 5, 929–932.
- Nishizuka, Y. (1988). The molecular heterogeneity of protein kinase C and its implications for cellular regulation. *Nature* 334, 661–665.
- Nishizuka, Y. (1992). Intracellular signaling by hydrolysis of phospholipids and activation of protein kinase C. *Science* 258, 607–614.
- O'Leary, J.L., Inukai, J., and Smith, J.M. (1971). Histogenesis of the cerebellar climbing fiber in the rat. *J. Comp. Neurol.* 142, 377–392.
- Palay, S.L., and Chan-Palay, V. (1974). *Cerebellar Cortex* (New York: Springer-Verlag).
- Rabacchi, S., Bailly, Y., Delhaye-Bouchaud, N., and Mariani, J. (1992). Involvement of the *N*-methyl *D*-aspartate (NMDA) receptor in synapse elimination during cerebellar development. *Science* 256, 1823–1825.
- Saito, N., Kikkawa, U., Nishizuka, Y., and Tanaka, C. (1988). Distribution of protein kinase C-like immunoreactive neurons in rat brain. *J. Neurosci.* 8, 369–382.
- Tanaka, C., and Nishizuka, Y. (1994). The protein kinase C family for neuronal signaling. *Annu. Rev. Neurosci.* 17, 551–567.
- Tanaka, C., and Saito, N. (1992). Localization of subspecies of protein kinase C in the mammalian central nervous system. *Neurochem. Int.* 21, 499–512.
- Watanabe, M., Mishina, M., and Inoue, Y. (1994). Distinct spatiotemporal expressions of five NMDA receptor channel subunit mRNAs in the cerebellum. *J. Comp. Neurol.* 343, 513–519.
- Woodward, D.J., Hoffer, B.J., and Altman, J. (1974). Physiological and pharmacological properties of Purkinje cells in rat cerebellum degranulated by postnatal X-irradiation. *J. Neurobiol.* 5, 283–304.
- Yamakuni, T., Usui, H., Iwanaga, T., Kondo, H., and Takahashi, Y. (1984). Isolation and immunohistochemical localization of a cerebellar protein. *Neurosci. Lett.* 45, 235–240.
- Yoshida, Y., Huang, F.L., Nakabayashi, H., and Huang, K.-P. (1988). Tissue distribution and developmental expression of protein kinase C isozymes. *J. Biochem. Chem.* 20, 9868–9873.
- Zucker, R.S. (1989). Short-term synaptic plasticity. *Annu. Rev. Neurosci.* 12, 13–31.